Check for updates

Phase I Clinical Trial of Prostate-Specific Membrane Antigen-Targeting ^{68}Ga-NGUL PET/CT in Healthy Volunteers and Patients with Prostate Cancer

Minseok Suh[1], Hyun Gee Ryoo[1, 2], Keon Wook Kang[1, 3], Jae Min Jeong[1], Chang Wook Jeong[4], Cheol Kwak[4], Gi Jeong Cheon[1, 3]

[1]Department of Nuclear Medicine, Seoul National University College of Medicine, Seoul, Korea; [2]Department of Nuclear Medicine, Seoul National University Bundang Hospital, Seongnam, Korea; [3]Cancer Research Institute, Seoul National University, Seoul, Korea; [4]Department of Urology, Seoul National University College of Medicine, Seoul, Korea

Objective: ^{68}Ga-NGUL is a novel prostate-specific membrane antigen (PSMA)-targeting tracer based on Glu-Urea-Lys derivatives conjugated to a 1,4,7-triazacyclononane-N,N',N''-triacetic acid (NOTA) chelator via a thiourea-type short linker. This phase I clinical trial of ^{68}Ga-NGUL was conducted to evaluate the safety and radiation dosimetry of ^{68}Ga-NGUL in healthy volunteers and the lesion detection rate of ^{68}Ga-NGUL in patients with prostate cancer.

Materials and Methods: We designed a prospective, open-label, single-arm clinical trial with two cohorts comprising six healthy adult men and six patients with metastatic prostate cancer. Safety and blood test-based toxicities were monitored throughout the study. PET/CT scans were acquired at multiple time points after administering ^{68}Ga-NGUL (2 MBq/kg; 96–165 MBq). In healthy adults, absorbed organ doses and effective doses were calculated using the OLINDA/EXM software. In patients with prostate cancer, the rates of detecting suspicious lesions by ^{68}Ga-NGUL PET/CT and conventional imaging (CT and bone scintigraphy) during the screening period, within one month after recruitment, were compared.

Results: All 12 participants (six healthy adults aged 31–32 years and six prostate cancer patients aged 57–81 years) completed the clinical trial. No drug-related adverse events were observed. In the healthy adult group, ^{68}Ga-NGUL was rapidly distributed, with the highest uptake in the kidneys. The median effective dose coefficient was calculated as 0.025 mSv/MBq, and cumulative activity in the bladder had the highest contribution. In patients with metastatic prostate cancer, 229 suspicious lesions were detected using either ^{68}Ga-NGUL PET/CT or conventional imaging. Among them, ^{68}Ga-NGUL PET/CT detected 199 (86.9%) lesions and CT or bone scintigraphy detected 114 (49.8%) lesions.

Conclusion: ^{68}Ga-NGUL can be safely applied clinically and has shown a higher detection rate for the localization of metastatic lesions in prostate cancer than conventional imaging. Therefore, ^{68}Ga-NGUL is a valuable option for prostate cancer imaging.

Keywords: *PSMA; Prostate cancer; ^{68}Ga-NGUL; PET/CT; Dosimetry*

INTRODUCTION

Prostate cancer is the second most common cancer among men worldwide. Although the incidence and mortality rates vary from country to country, the incidence rate is gradually increasing [1]. Prostate-specific membrane antigen (PSMA) is a membrane protein that specifically binds to epithelial cells of the prostate and is overexpressed in prostate cancer cells. PSMA is currently the most highlighted target for the diagnosis and treatment of prostate cancer [2,3]. To date, several PSMA-targeted agents have been developed, of which ^{68}Ga-PSMA-11 and ^{18}F-DCFPyl are the only Food and Drug Administration (FDA) approved imaging agents [4,5].

Our group has developed a novel ^{68}Ga labeled PSMA

targeting a PET tracer based on Glu-Urea-Lys (GUL) derivatives conjugated with a 1,4,7-triazacyclononane-N,N',N''-triacetic acid (NOTA) chelator via a thiourea-type short linker, named ^{68}Ga-NGUL [6]. Unlike conventional radio-pharmaceuticals, ^{68}Ga-NGUL lacks an amide bond in its structure. ^{68}Ga-NGUL can be considered more stable than tracers containing amide bonds because amide bonds are susceptible to degradation by proteolytic enzymes in the body [7]. In a head-to-head comparison study with ^{68}Ga-PSMA-11, ^{68}Ga-NGUL exhibited similar performance in detecting PSMA-avid lesions [8]. Thus, ^{68}Ga-NGUL can be considered a valuable option for PSMA-targeting PET/CT imaging and its theranostic applications. To further investigate the clinical feasibility and required step for clinical approval, we conducted a phase I clinical trial of ^{68}Ga-NGUL. The primary aim of this Phase I clinical trial was to evaluate the clinical safety and organ biodistribution-based radiation dosimetry of ^{68}Ga-NGUL in healthy volunteers. The secondary aim was to evaluate the lesion detection rate of ^{68}Ga-NGUL compared with conventional imaging modalities (CT and bone scintigraphy) in patients with prostate cancer.

MATERIALS AND METHODS

Participants

We designed a prospective, open-label, single-arm clinical trial with two cohorts comprising six healthy adult men as volunteers and six patients with metastatic prostate cancer. This study was authorized by the Korean Ministry of Food and Drug Safety (No. 202000493). Ethical approval was obtained from the Ethics Committee of the Hospital (IRB No. H-2006-121-1133), and all subjects provided written informed consent to receive ^{68}Ga-NGUL. The study was conducted in accordance with good clinical practice guidelines.

At the screening visit, those without clinically significant abnormalities in the medical history, electrocardiogram, clinical laboratory tests, physical examination, and those with prostate-specific antigen (PSA) levels of < 4.0 ng/mL were selected as healthy volunteers. Clinical laboratory tests included the following: white blood cell count (WBC), red blood cell count, platelet, WBC differential count, hemoglobin, hematocrit, glucose, blood urea nitrogen, creatinine, uric acid, total protein, albumin, alkaline phophatase, aspartate aminotransferas, alanine aminotransferse, γ-glutamyl transferase, total bilirubin, PSA, creatine kinase, Na, K, Cl, triglyceride, and total cholesterol.

Eligible patients were adults who had prostate cancer confirmed through tissue biopsy and those who met one of the following conditions: 1) patients with locally advanced prostate cancer (≥ T3a or Gleason score 8–10, or PSA > 20 ng/mL) who had not undergone radical prostatectomy and 2) those in whom metastatic lesions could be identified on radiological examination (CT, MRI, or bone scan). All enrolled patients met the second criterion. Those who had received anti-cancer radiation therapy for the identified prostate cancer lesion or had started a new anti-cancer drug regimen after the screening radiological examination were excluded from the study. The characteristics of the six patients with prostate cancer are summarized in Table 1.

To evaluate the safety of ^{68}Ga-NGUL administration, vital parameters, such as body temperature, blood pressure, and heart rate, were measured before injection, 3 hours after injection, and after 1 week. To determine toxicity, laboratory tests were performed 3 hours after administration and after 1 week. Adverse events were reported up to 1 week after injection, according to the Common Terminology Criteria for Adverse Events scoring system, version 4.0.

Preparation and Quality Control of ^{68}Ga-NGUL

^{68}Ga-NGUL was prepared as previously described [6].

Table 1. Characteristics of Patients with Prostate Cancer (n = 6)

	Age	Time Gap between Screening (Days)	PSA (ng/mL)	Status	Gleasons Score	Local Treatment	Chemotherapy	Hormonal Therapy
1	66	17	2885.0	mCRPC	5 + 4	Done	Done	Done
2	80	26	61.4	mCRPC	4 + 5	Done	Done	Done
3	75	28	10.1	mCRPC	4 + 4	Done	Not done	Done
4	73	66	0.74	mCRPC	5 + 4	Not done	Not done	Done
5	81	30	0.01	mHSPC	4 + 4	Not done	Not done	Done
6	57	60	0.23	mHSPC	5 + 5	Not done	Not done	Done

mCRPC = metastatic castration resistant prostate cancer, mHSPC = metastatic hormone sensitive prostate cancer, PSA = prostate-specific antigen

Briefly, ^{68}Ga chloride in 0.1 M hydrochloric acid solution was added to the NGUL kit vial (Cellbion). The vial was vigorously mixed for 1 minutes and incubated for 10 minutes at room temperature. Radiochemical purity was assessed according to the thin layer chromatography method using a 0.1 M sodium carbonate solution as a solvent with 1 µL of ^{68}Ga-NGUL. The radiochemical purity of ^{68}Ga-NGUL was greater than 95% and remained stable for 2 hours at room temperature.

Image Acquisition

For healthy adults, PET/CT scans were acquired 10 (± 5), 30 (± 10), 60 (± 10), 120 (± 20), and 180 (± 30) minutes after administration of ^{68}Ga-NGUL (2 MBq/kg; 96–165 MBq). Emission scans were acquired for 15 minutes using dedicated PET/CT scanners (Biograph mCT 64, Siemens Medical Solutions), followed by CT scans for attenuation correction. PET data were also corrected for dead time, random events, and scattering. PET images were reconstructed using an iterative algorithm (ordered-subset expectation maximization) with two iterations/21 subsets and Gauss-filtered to a transaxial resolution of 5 mm using the full width at half-maximum.

Patients with prostate cancer underwent PET/CT 60 (± 10) min and 120 (± 20) min after the administration of ^{68}Ga-NGUL (2 MBq/kg; 96–165 MBq). Reconstruction parameters were applied identically to healthy volunteers.

In normal controls, images were acquired at multiple time points for dosimetry analysis. In prostate cancer patients, images were acquired only at minimum time points to evaluate appropriate image timing and lesion detection ability.

Biodistribution

Normal organ distribution was evaluated in the aorta and in the following organs: bone (lumbar spine), kidneys, lacrimal glands, liver, lung, salivary glands, skeletal muscles (gluteal muscle), and spleen. Images were evaluated at each time point using MIM software (MIM Encore™, MIM Software Inc.). The volume of interest (VOIs) of the kidneys, liver, spleen, and L3-4 spines was drawn based on the CT scan. If there was metastasis in the L3-4 spine, VOIs were drawn on the other lumbar spine without metastasis. No visual evidence of tumor involvement was found in the other organs evaluated. The VOIs were applied to the salivary and lacrimal glands using a gradient-based segmentation method (PET edge). For the evaluation of

blood pool activity, circular regions of interest were drawn on the aorta, every 5-mm axial image, and interpolated to acquire a single VOI, from the liver tip to the subcarinal level. Spherical VOI was applied to the gluteal muscle to estimate skeletal muscle activity. Finally, the total-body contour was extracted using an embedded segmentation tool. Normal organ distribution and blood pool activity were quantified as the mean standardized uptake value (SUV_{mean}) in both healthy volunteers and prostate cancer patients.

Radiation Dosimetry

Radiation dosimetry was evaluated in healthy adults using the Medical Internal Radiation Dose (MIRD) S-value methodology [9]. The kidneys, liver, spleen, major salivary glands, urinary bladder, and the remaining parts of the body were selected as the source organs. Radiotracer activity in segmented volumes of interest was quantified as the percentage injected dose (%ID), and the time-activity curve was plotted for each source organ.

For each source organ (except the urinary bladder), mono-exponential or bi-exponential functions were iteratively fitted to the time-activity curve, and the subsequent residence time was calculated using the OLINDA/EXM software, version 1.1. The time-integrated activity coefficient in the urinary bladder was determined using the voiding bladder model in OLINDA/EXM with a voiding interval of 2 hours. The fraction of the tracer excreted through the bladder and the corresponding half-life were assessed according to the total body time-activity curve and biological half-life.

We evaluated the absorbed dose in various organs based on the male adult phantom model by entering the time-integrated activity coefficient of the source organs. The absorbed doses for the major salivary glands were determined using a spherical model to estimate the self-dose of the glands. The effective dose was calculated according to ICRP 103 [10].

Lesion Analysis

All scans were reviewed separately by nuclear medicine physicians blinded to the patient's medical history. In cases of inconsistency, consensus was reached. The number of suspected lesions and the location of each lesion were evaluated according to the results of conventional imaging modalities (CT and bone scintigraphy) at the time of screening and ^{68}Ga-NGUL PET/CT scans. The time interval between conventional imaging and ^{68}Ga-NGUL PET/CT was

set to a maximum of 1 month. A suspicious lesion in the ^{68}Ga-NGUL was defined as any soft tissue or skeletal lesion with a focal uptake that was higher than the blood pool and not explained by physiological uptake. The detection rates of ^{68}Ga-NGUL PET/CT and the conventional imaging modalities (CT and bone scintigraphy) were compared.

For quantitative analysis, PET images were normalized for the injected dose and body weight, and subsequently converted into SUV, defined as: (tracer concentration [kBq/mL])/(injected activity [kBq]/patient body weight [g]). The SUV_{max} (highest voxel SUV value within the segmented tumor) and SUV_{mean} (average SUV value of all voxels within
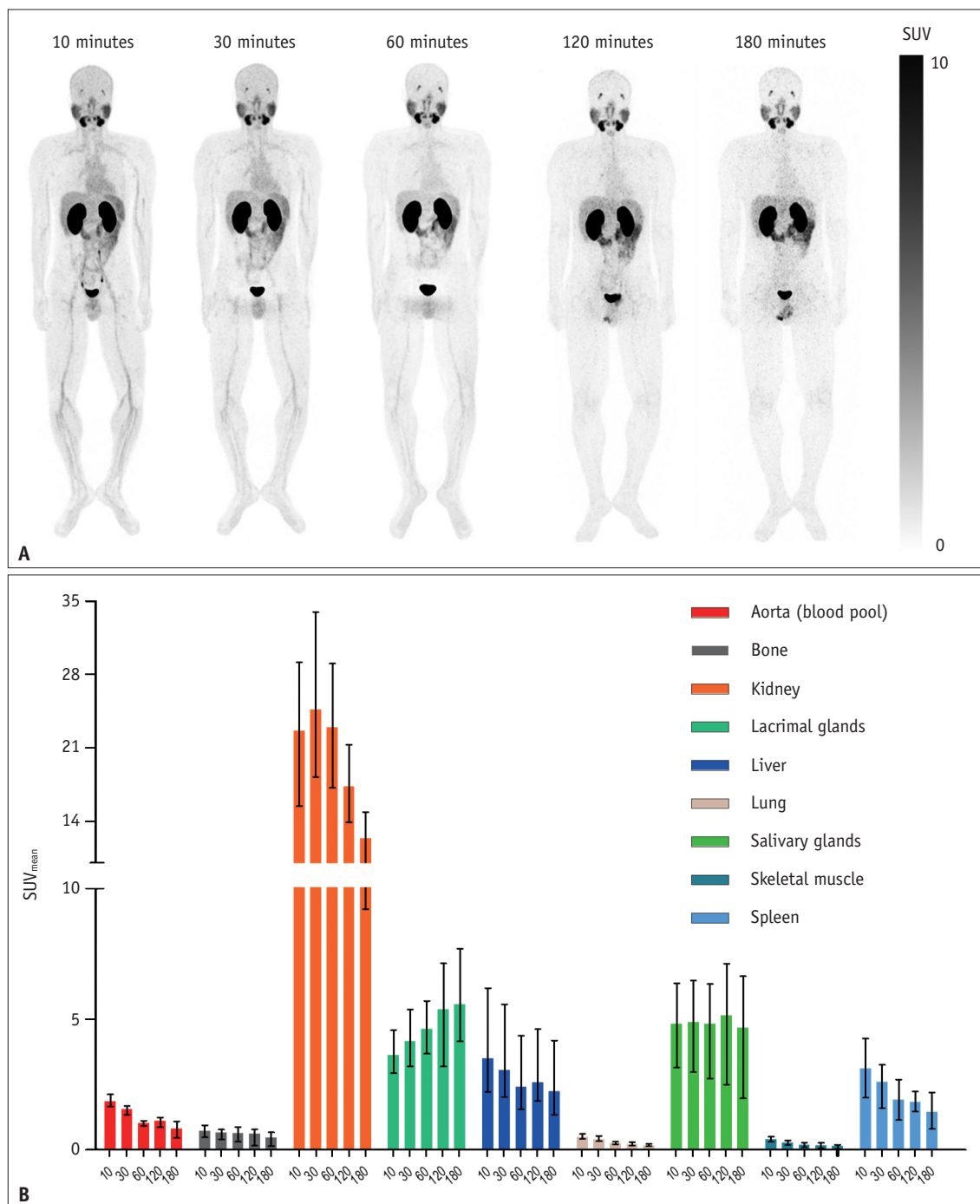
Fig. 1. Biodistribution of ^{68}Ga-NGUL.
A. Maximum-intensity projection PET images of a representative healthy subject, scaled as specified by the SUV color bar (SUV between 0 and 10). **B.** Average radioactivity of ^{68}Ga-NGUL in each organ presented as the SUV_{mean} at each time point. SUV = standard uptake value

the segmented tumor) of all lesions, up to a maximum of five lesions (and a maximum of two lesions per organ) with the most intense tracer uptake, were estimated for each patient. The gradient-based method (PET edge) was applied for lesion segmentation using the MIM software. Lesions with low uptake were manually adjusted after applying the PET edge. The tumor-to-background ratio was measured based on the ratio of the tumor SUV_{mean} to the blood pool (aorta) SUV_{mean}, reflecting the background activity.

Statistical Analysis

Statistical analyses were performed using the PRISM (version 5.0; GraphPad Software) and MedCalc statistical packages version 14.8 (MedCalc Statistical Software). A comparison of normal organ biodistribution between healthy volunteers and patients with prostate cancer was performed using the Mann–Whitney U test. Lesion detection was compared between ^{68}Ga-NGUL and conventional imaging using Fisher's exact test. Statistical significance was set at $p < 0.05$.

RESULTS

Adverse Events

All 12 participants (six healthy adults aged 31–32 years and six prostate cancer patients aged 57–81 years) completed the clinical trial. All patients tolerated the test well, and no drug-related adverse events were observed. All the observed vital parameters remained within the normal range, with no significant changes before and after the test. Blood samples analyzed for hematology and biochemistry indicated no significant change after injection and remained within subject biological variability.

Normal-Organ Biodistribution

Maximum-intensity projection PET images of healthy volunteers at each time point are shown in Figure 1A. In the 10-minutes image, ^{68}Ga-NGUL was rapidly removed from the blood and distributed to the kidneys, salivary glands, lacrimal glands, liver, spleen, and small bowel. Kidney uptake peaked at 30 minutes and then gradually decreased; uptake from the liver and spleen also decreased with time. ^{68}Ga-NGUL uptake in the lacrimal glands and salivary glands tended to increase and remain constant, respectively (Fig. 1B). Based on the evaluation of the total body activity, up to 30% of the injected activity was cleared through the urinary system within 3 hours.

In both healthy subjects and patients with prostate cancer, ^{68}Ga-NGUL showed the highest uptake in the kidney, followed by the salivary glands, lacrimal glands, liver, and spleen 60 minutes after administration (Fig. 2). However, the kidneys of patients with prostate cancer showed significantly lower uptake than those of healthy volunteers ($p = 0.002$). ^{68}Ga-NGUL uptake in the salivary and lacrimal glands also tended to be lower than that in healthy volunteers, although the difference was not statistically significant.

Radiation Dosimetry

The mean absorbed dose for each organ and mean effective dose are summarized in Table 2. The organ with the highest absorbed dose was the urinary bladder wall (0.401 mGy/MBq), followed by the kidneys (0.332 mGy/MBq), salivary glands (0.051 mGy/MBq), liver (0.024 mGy/MBq), and spleen (0.022 mGy/MBq). The median effective dose was 0.025 mSv/MBq (interquatile range 0.021–0.029), and based on the evaluation of the actual administered dose, the median effective dose was 3.66 mSv.

Lesion Analysis

Overall, 229 suspicious lesions (13 hepatic and 216 bone lesions) were identified using either ^{68}Ga-NGUL PET/CT or conventional imaging. An example is shown in Figure 3. The
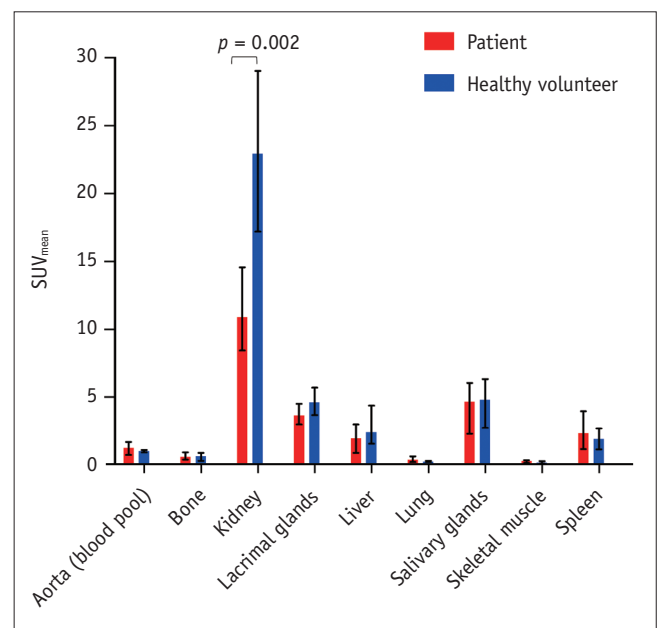
Fig. 2. Comparison of radioactivity (SUV_{mean}) of each organ between patients with prostate cancer and healthy volunteers at 60 minutes after the administration of ^{68}Ga-NGUL.
SUV = standard uptake value

Table 2. Summary of Dosimetry Results

Organs	Median Absorbed Dose (mGy/MBq)	Interquartile Range
Adrenals	0.011	0.010–0.012
Brain	0.005	0.005–0.005
Breasts	0.005	0.005–0.005
Gallbladder wall	0.010	0.009–0.010
Lower large intestine wall	0.012	0.010–0.014
Small intestine	0.010	0.008–0.010
Stomach wall	0.008	0.007–0.008
Upper large intestine wall	0.009	0.008–0.009
Heart wall	0.007	0.006–0.009
Kidneys	0.326	0.293–0.374
Liver	0.023	0.018–0.030
Lungs	0.011	0.006–0.017
Muscle	0.008	0.007–0.008
Pancreas	0.009	0.009–0.010
Red marrow	0.007	0.006–0.007
Osteogenic cells	0.009	0.008–0.010
Skin	0.005	0.005–0.006
Spleen	0.022	0.018–0.027
Testes	0.009	0.007–0.011
Thymus	0.006	0.005–0.006
Thyroid	0.005	0.005–0.005
Urinary bladder wall	0.379	0.321–0.505
Salivary glands	0.046	0.043–0.059
Effective dose (mSv/MBq)	0.025	0.021–0.029

detection rates of ^{68}Ga-NGUL and conventional imaging (CT and bone scintigraphy) were 86.9% (199/229) and 49.8% (114/229), respectively ($p < 0.001$) (Table 3).

Quantitative uptake was evaluated in 11 lesions (two lesions of liver metastases and nine lesions of bone metastases). The quantified uptake in metastatic lesions between 60 and 120 minutes after ^{68}Ga-NGUL administration demonstrated a significant increase in SUV_{max} and SUV_{mean} by approximately 15% (Fig. 4A, B). However, the tumor-to-background ratio, defined by blood pool uptake as a background, showed no significant change between 60 and 120 minutes (Fig. 4C).

DISCUSSION

Administration of ^{68}Ga-NGUL was well tolerated without demonstrable drug-related adverse events in both healthy volunteers and patients with prostate cancer, and showed superior lesion detection rates compared with conventional imaging studies. In healthy volunteers, ^{68}Ga-NGUL was readily distributed along the kidneys, salivary glands,

lacrimal glands, liver, and spleen, and was rapidly excreted through the urinary system. Correspondingly, the highest absorbed dose was observed in the urinary bladder wall, followed by the kidney. The detection rate of ^{68}Ga-NGUL for suspicious lesions was higher than that of conventional imaging modalities including CT and bone scintigraphy. Although the lesion uptake of ^{68}Ga-NGUL was higher 120 minutes after administration, the tumor-to-background ratio showed no significant difference between 60 and 120 minutes. Therefore, considering practical issues, we recommend scanning the patients 60 minutes after administration.

^{68}Ga-NGUL contains a matching therapeutic agent based on the same GUL derivative conjugated with a DOTA chelator, "^{177}Lu-DGUL". Currently, ^{177}Lu-DGUL is under phase 1/2 clinical trials aimed at evaluating its safety, tolerability, dosimetry, and efficacy in patients with metastatic castration-resistant prostate cancer refractory to standard therapy. Among the therapeutic agents targeting PSMA, ^{177}Lu-PSMA-617 is currently at the forefront for clinical approval and application [11-13]. The most widely used companion imaging agent for ^{177}Lu-PSMA-617 is the ^{68}Ga-PSMA-11 scan. However, PSMA-617 has been reported to have slower tumor accumulation and clearance kinetics than PSMA-11 [14]. Fluorine-18-based PSMA imaging agents can also be used; however, DCFPyl, which is currently the most widely used imaging agent, has different kinetics than PSMA-617 [15]. Such differences in kinetics and biodistribution may limit the optimal selection of patients for ^{177}Lu-PSMA-617 therapy. On the other hand, ^{68}Ga-NGUL, based on the targeting motif identical to that of ^{177}Lu-DGUL, is expected to show the same distribution and kinetics [6]. As a result, ^{68}Ga-NGUL is expected to be an optimal companion imaging method for ^{177}Lu-DGUL.

As previously reported in a comparative study of ^{68}Ga-PSMA-11, rapid urinary excretion of ^{68}Ga-NGUL was observed [8]. Accordingly, it was estimated that the urinary bladder wall had the highest absorbed dose. According to the FDA label, the absorbed dose of the bladder wall is approximately four times higher than that of PSMA-11 (NGUL vs. PSMA-11: 0.401 mGy/MBq vs. 0.098 mGy/MBq) [16]. However, the level of radiation exposure in ^{68}Ga-NGUL PET/CT examinations is reasonably low, approximately 3–4 times the annual natural background exposure worldwide [17]. Radiotracer activity in the bladder majorly contributed to effective dose, and for this reason, the effective dose was also relatively higher than that of PSMA-11 (0.025
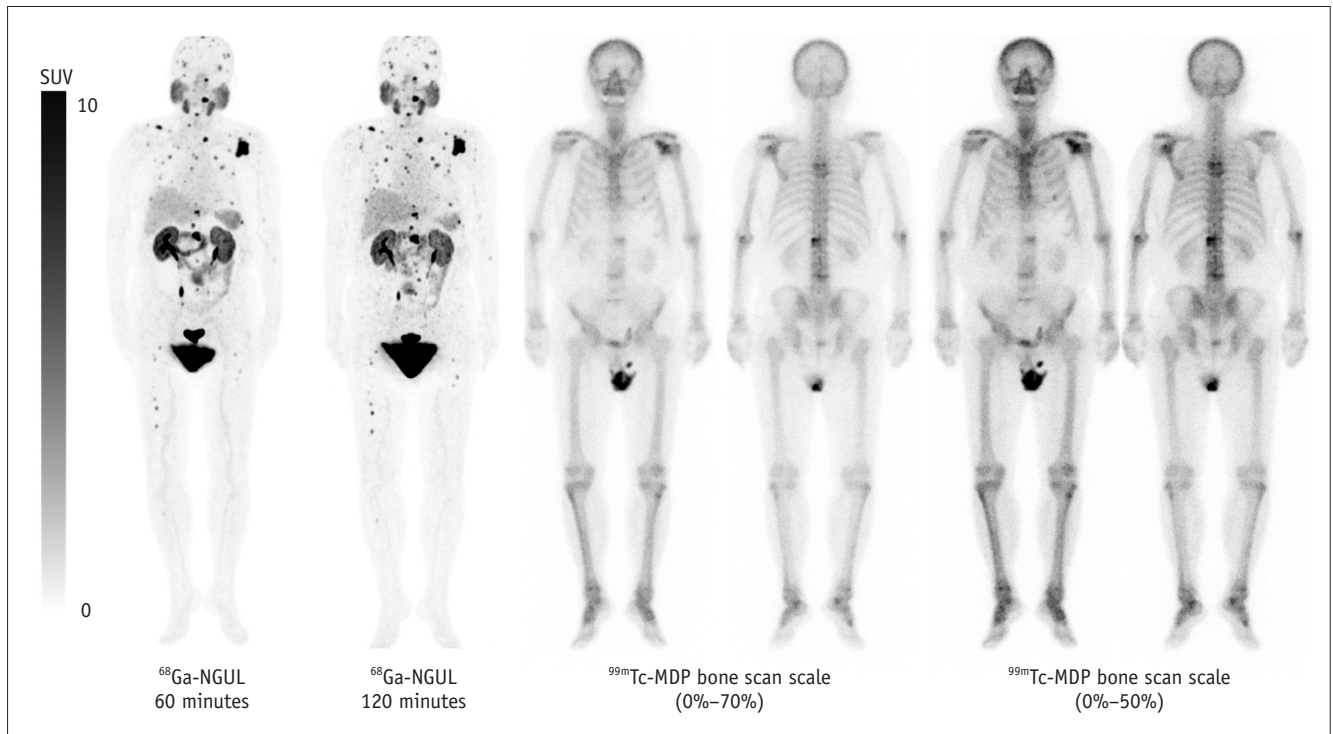
Fig. 3. Maximum-intensity projection ⁶⁸Ga-NGUL PET images (at 60 and 120 minutes after administration) and ⁹⁹ᵐTc-MDP bone scintigraphy images (with different intensity scale) of the 80-year-old patient with metastatic castration-resistant prostate cancer (patient #2). The time gap between the two scans was 26 days. MDP = methylene diphosphonate

Table 3. Summary of Lesion Detection Rate for 229 Metastatic Lesions

Patient	Number of Lesions Detected						Detection Rate (%)	
	Bone		Liver		Total			
	NGUL	Bone Scintigraphy	NGUL	CT	NGUL	Conventional Imaging	NGUL	Conventional Imaging
1	84	64	13	12	97	76	100	78.4
2	97	5	0	0	97	5	98	5
3	1	1	0	0	1	1	100	100
4	1	18	0	0	1	18	5.6	100
5	1	1	0	0	1	1	100	100
6	2	13	0	0	2	13	15.4	100
Sum	186	102	13	12	199	114	86.9	49.8

mSv/MBq vs. 0.017 mSv/MBq). However, exposure to other organs, including the kidney (0.332 mGy/MBq vs. 0.371 mGy/MBq) and spleen (0.022 mGy/MBq vs. 0.065 mGy/MBq), was lower than that of ⁶⁸Ga-PSMA-11, which is in line with the results of a previous comparative study [8]. The lower molecular weight (769.82 g/mol vs. 947 g/mol) and higher hydrophilicity (log P = -3.3 vs. -3.9) of ⁶⁸Ga-NGUL compared with ⁶⁸Ga-PSMA-11 may explain the difference in the urinary excretion. Both adequate hydration and frequent bladder emptying are necessary to reduce radiation exposure and urinary tract uptake, which may interfere with the detection of adjacent lesions.

Previous studies on ⁶⁸Ga-PSMA-11 have shown that PSMA imaging is superior to conventional imaging modalities in staging and detecting biochemical failure in patients with prostate cancer [18,19]. In particular, ⁶⁸Ga-PSMA-11 PET/CT was superior in detecting nodal and distant metastatic lesions than conventional imaging, including CT and bone scans, in a recent prospective, multicenter, randomized study [19]. In line with previous studies, ⁶⁸Ga-NGUL showed an overall higher lesion detection rate than conventional imaging. However, the tumor detection rate and SUV_max differed according to patient characteristics. Patients with high PSA levels (patients #1, #2, and #3) showed a
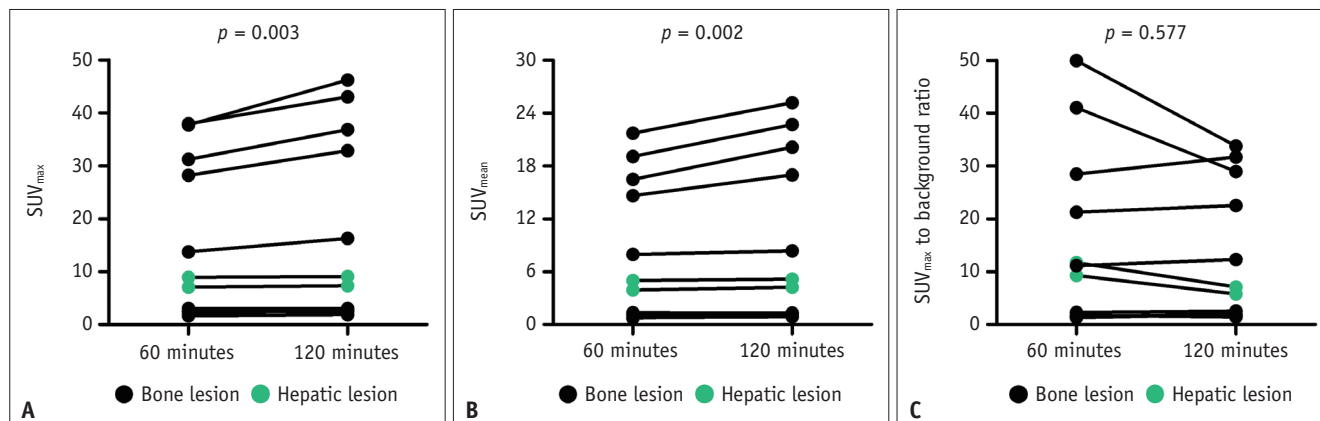
Fig. 4. Comparison of quantitative values of 11 lesions at 60 and 120 minutes after the administration of ^{68}Ga-NGUL. SUV_{max} **(A)**, SUV_{mean} **(B)**, and SUV_{max} **(C)** to background (blood pool) ratio. SUV = standard uptake value

higher overall detection rate and tumor SUV_{max} than those with lower PSA levels (patients #4, #5, and #6). This difference is consistent with the well-known results that PSMA-avid tumor burden is significantly associated with PSA levels [20,21]. Using the Spearman rank test, we also found a significant correlation between the tumor SUV_{max} and PSA levels (Supplementary Fig. 1). Moreover, in the group with low PSA levels, two patients (patients #5 and #6) had metastatic hormone-sensitive prostate cancer, whose disease was well controlled and showed a decrease in the PSA level compared with the immediate preceding test, which may be the reason for the low PSMA avidity. In summary, ^{68}Ga-NGUL has superior lesion detection ability compared to conventional imaging, especially bone scintigraphy, and the tumor SUV_{max} is affected by the PSA level.

This study had certain limitations. First, owing to the small number of patients, we cannot draw a generalized conclusion. A phase 2/3 trial with many patients is warranted to establish the efficacy of ^{68}Ga-NGUL for the detection of PSMA-positive prostate cancer. Second, because the purpose of this clinical trial was focused on dosimetry and safety, the patient group was recruited based on a criterion with a relatively long period between screening images and ^{68}Ga-NGUL scans (mean, 38 days). Evaluation of the efficacy of ^{68}Ga-NGUL by applying a stricter indication is required in future clinical trials. Finally, there are limitations to applying the MIRD S-value methodology for dosimetry analysis. This method assumes that radioactivity is evenly distributed throughout the body immediately after administration, and any unmeasured radioactivity is assigned to the remainder of the body. However, this assumption is difficult to apply in actual clinical practice.

Voxel-based dosimetry may overcome these limitations and a more accurate dose profile can be obtained [22].

In conclusion, ^{68}Ga-NGUL was well tolerated without drug-related adverse events and showed a reasonably low radiation exposure. We suggest an optimal ^{68}Ga-NGUL image acquisition time of 60 minutes after administration. ^{68}Ga-NGUL PET/CT showed superiority over conventional imaging in detecting metastatic lesions, and it is necessary to consolidate its diagnostic efficacy through further studies. Accordingly, ^{68}Ga-NGUL could be a valuable option for PSMA imaging and theranostics.

Supplement

The Supplement is available with this article at https://doi.org/10.3348/kjr.2022.0176.

Investigation: all authors. Methodology: Minseok Suh, Hyun Gee Ryoo, Keon Wook Kang, Jae Min Jeong, Gi Jeong Cheon. Project administration: Chang Wook Jeong, Cheol Kwak, Gi Jeong Cheon. Supervision: Keon Wook Kang, Jae Min Jeong, Chang Wook Jeong, Cheol Kwak, Gi Jeong Cheon. Validation: Minseok Suh, Hyun Gee Ryoo. Visualization: Minseok Suh, Hyun Gee Ryoo. Writing—original draft: Minseok Suh, Hyun Gee Ryoo. Writing—review & editing: Keon Wook Kang, Jae Min Jeong, Chang Wook Jeong, Cheol Kwak, Gi Jeong Cheon.

ORCID iDs
Minseok Suh
  https://orcid.org/0000-0002-6932-8552
Hyun Gee Ryoo
  https://orcid.org/0000-0001-5020-5846
Keon Wook Kang
  https://orcid.org/0000-0003-2622-9017
Jae Min Jeong
  https://orcid.org/0000-0003-2611-6020
Chang Wook Jeong
  https://orcid.org/0000-0002-2200-5019
Cheol Kwak
  https://orcid.org/0000-0002-1987-2111
Gi Jeong Cheon
  https://orcid.org/0000-0002-1360-5186

Funding Statement
This work was funded by Cellbion Co., Ltd. (Seoul, Korea). This work was supported by the Technology Innovation Program (20001235, Development of Novel Radiopharmaceutical for Prostate Cancer Targeted Imaging Diagnosis) funded By the Ministry of Trade, Industry & Energy (MI, Korea) and the National Research Foundation of Korea (NRF) grant funded by the Korean Government (MSIT) (No. 2020M2D9A1093988).

REFERENCES

1. Rawla P. Epidemiology of prostate cancer. *World J Oncol* 2019;10:63-89
2. Oh SW, Cheon GJ. Prostate-specific membrane antigen PET imaging in prostate cancer: opportunities and challenges. *Korean J Radiol* 2018;19:819-831
3. Fütterer JJ, Nagarajah J. Research highlight: 68Ga-PSMA-11 PET imaging for pelvic nodal metastasis in prostate cancer. *Korean J Radiol* 2022;23:293-294
4. Carlucci G, Ippisch R, Slavik R, Mishoe A, Blecha J, Zhu S. 68Ga-PSMA-11 NDA approval: a novel and successful academic partnership. *J Nucl Med* 2021;62:149-155
5. Morris MJ, Rowe SP, Gorin MA, Saperstein L, Pouliot F, Josephson D, et al. Diagnostic performance of 18F-DCFPyL-PET/CT in men with biochemically recurrent prostate cancer: results from the CONDOR phase III, multicenter study. *Clin Cancer Res* 2021;27:3674-3682
6. Moon SH, Hong MK, Kim YJ, Lee YS, Lee DS, Chung JK, et al. Development of a Ga-68 labeled PET tracer with short linker for prostate-specific membrane antigen (PSMA) targeting. *Bioorg Med Chem* 2018;26:2501-2507
7. Evans BJ, King AT, Katsifis A, Matesic L, Jamie JF. Methods to enhance the metabolic stability of peptide-based PET radiopharmaceuticals. *Molecules* 2020;25:2314
8. Suh M, Im HJ, Ryoo HG, Kang KW, Jeong JM, Prakash S, et al. Head-to-head comparison of 68Ga-NOTA (68Ga-NGUL) and 68Ga-PSMA-11 in patients with metastatic prostate cancer: a prospective study. *J Nucl Med* 2021;62:1457-1460
9. Bolch WE, Eckerman KF, Sgouros G, Thomas SR. MIRD pamphlet No. 21: a generalized schema for radiopharmaceutical dosimetry--standardization of nomenclature. *J Nucl Med* 2009;50:477-484
10. ICRP. The 2007 recommendations of the international commission on radiological protection. ICRP publication 103. *Ann ICRP* 2007;37:1-332
11. Hofman MS, Emmett L, Sandhu S, Iravani A, Joshua AM, Goh JC, et al. [¹⁷⁷Lu]Lu-PSMA-617 versus cabazitaxel in patients with metastatic castration-resistant prostate cancer (TheraP): a randomised, open-label, phase 2 trial. *Lancet* 2021;397:797-804
12. Hofman MS, Violet J, Hicks RJ, Ferdinandus J, Thang SP, Akhurst T, et al. [¹⁷⁷Lu]-PSMA-617 radionuclide treatment in patients with metastatic castration-resistant prostate cancer (LuPSMA trial): a single-centre, single-arm, phase 2 study. *Lancet Oncol* 2018;19:825-833
13. Morris MJ, De Bono JS, Chi KN, Fizazi K, Herrmann K, Rahbar K, et al. Phase III study of lutetium-177-PSMA-617 in patients with metastatic castration-resistant prostate cancer (VISION). *J Clin Oncol* 2021;39:LBA4
14. Afshar-Oromieh A, Hetzheim H, Kratochwil C, Benesova M, Eder M, Neels OC, et al. The theranostic PSMA ligand PSMA-617 in the diagnosis of prostate cancer by PET/CT: biodistribution in humans, radiation dosimetry, and first evaluation of tumor lesions. *J Nucl Med* 2015;56:1697-1705
15. Szabo Z, Mena E, Rowe SP, Plyku D, Nidal R, Eisenberger MA, et al. Initial evaluation of [18F]DCFPyL for prostate-specific membrane antigen (PSMA)-targeted PET imaging of prostate cancer. *Mol Imaging Biol* 2015;17:565-574
16. University of California Los Angeles. Ga 68 PSMA-11 [package insert]. accessdata.fda.gov Web site. www.accessdata.fda.gov/drugsatfda_docs/label/2020/212642s000lbl.pdf. Accessed May 15, 2021
17. Thorne MC. Background radiation: natural and man-made. *J Radiol Prot* 2003;23:29-42

18. Eiber M, Maurer T, Souvatzoglou M, Beer AJ, Ruffani A, Haller B, et al. Evaluation of hybrid 68Ga-PSMA ligand PET/CT in 248 patients with biochemical recurrence after radical prostatectomy. *J Nucl Med* 2015;56:668-674

19. Hofman MS, Lawrentschuk N, Francis RJ, Tang C, Vela I, Thomas P, et al. Prostate-specific membrane antigen PET-CT in patients with high-risk prostate cancer before curative-intent surgery or radiotherapy (proPSMA): a prospective, randomised, multicentre study. *Lancet* 2020;395:1208-1216

20. Ceci F, Uprimny C, Nilica B, Geraldo L, Kendler D, Kroiss A, et al. (68)Ga-PSMA PET/CT for restaging recurrent prostate cancer: which factors are associated with PET/CT detection rate? *Eur J Nucl Med Mol Imaging* 2015;42:1284-1294

21. Schmidkonz C, Cordes M, Schmidt D, Bäuerle T, Goetz TI, Beck M, et al. 68Ga-PSMA-11 PET/CT-derived metabolic parameters for determination of whole-body tumor burden and treatment response in prostate cancer. *Eur J Nucl Med Mol Imaging* 2018;45:1862-1872

22. Gupta A, Shin JH, Lee MS, Park JY, Kim K, Kim JH, et al. Voxel-based dosimetry of iron oxide nanoparticle-conjugated 177Lu-labeled folic acid using SPECT/CT imaging of mice. *Mol Pharm* 2019;16:1498-1506